Time-dependent renormalized Redfield theory II for off-diagonal transition in reduced density matrix

Akihiro Kimura

Department of Physics, Graduate School of Science, Nagoya University, Furo-cho, Chikusa-ku, Nagoya, Japan, 464-8602

Abstract

In our previous letter (A. Kimura, Chem. Phys. Lett. 645 (2016) 123), we constructed time-dependent renormalized Redfield theory (TRRT) only for diagonal transition in a reduced density matrix. In this letter, we formulate the general expression for off-diagonal transition in the reduced density matrix. We discuss the applicability of TRRT by numerically comparing the dependencies on the energy gap of the exciton relaxation rate by using the TRRT and the modified Redfield theory (MRT). In particular, we roughly show that TRRT improves MRT for the detailed balance about the excitation energy transfer reaction.

Keywords:
Redfield theory, Exciton, Polaron, Quantum master equation

1. Introduction

Photosynthesis converts photo-energy into bio-energy in the form of carbohydrates. In the initial stages of photosynthesis, immediately following the absorption of photons, the electronically excited state of chlorophyll in the antenna protein is transferred to a reaction center with high quantum yield through strategies that remain unknown. The quantum effect of excitation energy transfer in the antenna system has recently been reported [1–3]. In particular, long-lasting quantum coherence via nuclear vibrations in photosynthetic antennas at room temperature has been the focus of research, and has been treated experimentally as well as theoretically [4].

When exciton coupling strength V^e is much smaller than the reorganization energy λ as $V^e \ll \lambda$, the localized excitation state as the donor molecule transfers to an energetically lower exciton state as the acceptor molecule. The excitation transfer rate has been expressed by Förster [5]. In the opposite limiting case ($V^e \gg \lambda$), the exciton state delocalizes in the system, and the relaxation process to the energetically lower delocalized exciton states occurs. The relaxation process can be expressed by Redfield theory [6].

While such a limiting case is easily treatable using a simple perturbation method, it is difficult to apply the perturbation method to it, especially in the case of intermediate coupling [4, 7]. For such situations, Zhang et al. modified Redfield theory. The modified Redfield theory (MRT) treats electronic off-diagonal elements in exciton-phonon interaction as a perturbation term [8, 9]. In recent theoretical developments, a coherent modified Redfield theory (CMRT) was constructed by Hwang-Fu et al. [10, 11] and was applied to the analysis of the energy transfer pathway in photosynthetic antenna systems [12].

We recently constructed a time-dependent renormalized Redfield theory (TRRT) and derived a formula to represent the exciton relaxation rate [13]. However, the rate formula could not analyze the physics of quantum coherence in such photosynthetic antenna systems due to the rate formula between the diagonal elements of the reduced density matrix element for delocalized exciton representation. Hence, in this letter, we extend the formalism of the previously expressed rate to analyze the transition rate between off-diagonal elements in the system.

The quantum master equation for the reduced density matrix element under second-order perturbative approximation by interaction representation is expressed by using the Nakajima-Zwanzig equation as [14, 15]

$$i\hbar\frac{\partial\mathcal{P}\rho_I(t)}{\partial t} = \mathcal{P}[V_I(t), \mathcal{Q}\rho_I(0)] + \mathcal{P}[V_I(t), \mathcal{P}\rho_I(t)] - \frac{i}{\hbar}\int_0^t dt'\mathcal{P}[V_I(t), \mathcal{Q}[V_I(t'), \mathcal{P}\rho_I(t')] \quad (1)$$

where $\mathcal{P}$ is the projection operator $\mathcal{P}A \equiv \rho_b \mathrm{Tr}[A]$. ρ_b is expressed as $e^{-\beta H_B}/\mathrm{Tr}[e^{-\beta H_B}]$. H_B is phonon-bath Hamiltonian. The operator $V_I(t)$ is perturbative Hamiltonian with interaction representation defined as $e^{iH_0 t/\hbar} V e^{-iH_0 t/\hbar}$. The first term on the rhs is an inhomogeneous term, which can be neglected due to proper initial conditions obtaining in the reduced density matrix. The third term of rhs represent dissipation, which is expressed by the time correlation of the perturbative Hamiltonian with interaction representation $V_I(t)$. The second term of the rhs has been neglected by comparing the result according to the quantum master equation with that obtained by using numerically exact calculation. This elimination simplifies the equation of motion. However, it cannot be easily justified [16]. By using the renormalization approach, the time correlation function in the dissipation term of the quantum master equation becomes the formalism of the variance-covariance matrix. However, in

Email address: akimura@tb.phys.nagoya-u.ac.jp (Akihiro Kimura)

case of interaction representation for the quantum master equation, it is difficult to analyze the temporal propagation of the reduced matrix element by Schrödinger representation. The CMRT overcomes this problem by dividing the quantum master equation into a coherent term and a dissipation term. The time-dependent renormalization approach in this letter improves the dissipation term in the CMRT.

In the remainder of this letter, the model Hamiltonian and analytical strategies are stated in Section 2. The requisite numerical analysis is conducted in Section 3. In Section 4, we discuss some findings and the conclusions that can be drawn from them. The details of the analytical expression are presented in the Appendix.

2. Theory

2.1. Hamiltonian

Let us define the total Hamiltonian of the system. We express the ket vector $|n\rangle$ as the electronic excited state at the nth site, where the electronic site energy is E_n. The exciton coupling strength between the nth and mth molecules is expressed by V^e_{nm}. We introduce the pure exciton Hamiltonian as $[\sum_n E_n|n\rangle\langle n| + \sum_{n\neq m} V^e_{nm}[|n\rangle\langle m| + |m\rangle\langle n|]]|\mu\rangle = E_\mu|\mu\rangle$ where $|\mu\rangle$ is the ket vector in the pure exciton representation expressed by the site representation as

$$|\mu\rangle = \sum_n C^\mu_n|n\rangle. \tag{2}$$

For nuclear motion, we only consider the phonon bath, where the creation (annihilation) operator for the kth phonon mode is expressed as $b^\dagger_k$ (b_k), the frequency of which is ω_k. Finally, g_{nk} is introduced as the exciton-phonon coupling strength at the nth excited state: We introduce exciton-phonon coupling using pure exciton representation as

$$G^{\mu\nu}_k = \sum_n C^\mu_n C^\nu_n g_{nk}. \tag{3}$$

Hence, the total Hamiltonian based on pure exciton representation can be expressed as $H = H_0 + V$

$$H = H_0 + V, \tag{4}$$

$$H_0 = \sum_\mu [E_\mu + H_B + B_{\mu\mu}]|\mu\rangle\langle\mu|, \tag{5}$$

$$V = \sum_{\mu\neq\nu} B_{\mu\nu}|\mu\rangle\langle\nu|, \tag{6}$$

where $H_B = \sum_k \hbar\omega_k b^\dagger_k b_k$ is the phonon-bath Hamiltonian. Here, $B_{\mu\nu}$ is defined as

$$B_{\mu\nu} = \sum_k G^{\mu\nu}_k (b^\dagger_k + b_k). \tag{7}$$

We now introduce the shift operator $\theta \equiv e^S$, where S is defined as

$$S = \sum_\mu S_{\mu\mu} = \sum_{\mu k} \frac{G^{\mu\mu}_k}{\hbar\omega_k}(b^\dagger_k - b_k)|\mu\rangle\langle\mu|. \tag{8}$$

Using the shift operator, we apply a unitary transformation from Eq. (4) to the total Hamiltonian as $\theta H\theta^\dagger = H^R_0(t) + V^R(t)$ as in the section 2.3.

2.2. Renormalization Strategy

We divide the total Hamiltonian H into two parts, renormalized non-perturbative Hamiltonian and its perturbative Hamiltonian as $H^R_0(t) + V^R(t)$, in advance. Based on the zeroth-order propagator $U(t_o)$ as $\exp_+\left[-\frac{i}{\hbar}\int_0^t dt_1 H^R_0(t_1)\right]$, by re-introducing the shift operator, we obtain a first-order expansion of the unitary-transformed propagator $e^{-iHt/\hbar}$ as

$$\begin{aligned}\langle f|\theta^\dagger e^{-iHt/\hbar}\theta|i\rangle =& \langle f|\theta^\dagger U(t)\theta|i\rangle \\ &- \frac{i}{\hbar}\int_0^t dt_1 \langle f|\theta^\dagger U(t) V^R_I(t_1)\theta|i\rangle,\end{aligned} \tag{9}$$

where we take the element in the electronic state, and $V^R_I(t)$ is the interaction representation of $V^R(t)$, defined as $U^\dagger(t)V^R(t)U(t)$.

The reduced density operator is expressed as

$$\rho(t) = \mathrm{Tr}[\langle f|\theta^\dagger e^{-iHt/\hbar}\theta|i\rangle\rho_b\langle i'|\theta^\dagger e^{iHt/\hbar}\theta|f'\rangle], \tag{10}$$

where ρ_b is defined as $e^{-\beta H_B}/\mathrm{Tr}[e^{-\beta H_B}]$. Inserting Eq. (9) into Eq. (10), we obtain

$$\begin{aligned}\rho(t) =& \langle 1, 1\rangle_t - \frac{i}{\hbar}\int_0^t dt_1[\langle 1, V^R_I(t_1)\rangle_t - \langle V^{R\dagger}_I(t_1), 1\rangle_t] \\ &+ \frac{1}{\hbar^2}\int_0^t dt_1 \int_0^t dt'_1 \langle V^{R\dagger}_I(t'_1), V^R_I(t_1)\rangle_t,\end{aligned} \tag{11}$$

where we introduce the new bracket as

$$\langle A, B\rangle_t \equiv \mathrm{Tr}[\langle i'|\theta^\dagger A U^\dagger(t)\theta|f'\rangle\langle f|\theta^\dagger U(t) B\theta|i\rangle\rho_b]. \tag{12}$$

Apparently, in order to eliminate the first order term of the rhs in Eq. (11), we need to introduce the average interaction Hamiltonian, which is independent of the phonon operator but depends on the electronic exciton states. In addition, the average interaction Hamiltonian needs to be a function of two type variables for time. One is the integral variable t_1; the other is the artificially observing time t. Hence, we redefine renormalized non-perturbative Hamiltonian $H^R_0(t_1) \equiv H_0(t_1) + v_c(t_1, t)$, and renormalized perturbative Hamiltonian as $V^R(t_1) \equiv V_0(t_1) - v_c(t_1, t)$. The average matrix element $v_c(t, t_1)$ is determined to satisfy the relation as $\langle 1, V^R_I(t_1)\rangle_t = \langle V^{R\dagger}_I(t_1), 1\rangle_t = 0$

2.3. Renormalized Hamiltonian

Introducing the c-number as the strength of time-dependent interaction $v_{c\mu\nu}(t, t')$ and the renormalized exciton state $|\alpha(t)\rangle$ as below, we define the non-perturbative renormalized Hamiltonian H^R_0 as

$$H^R_0(t) = \sum_\alpha [\epsilon'_\alpha(t) + H_B]|\alpha(t)\rangle\langle\alpha(t)|, \tag{13}$$

$$[\sum_\mu \epsilon_\mu|\mu\rangle\langle\mu| + \sum_{\mu\nu}^{\mu\neq\nu} v_{c\mu\nu}(t, t')|\mu\rangle\langle\nu|]|\alpha(t)\rangle = \epsilon'_\alpha(t)|\alpha(t)\rangle, \tag{14}$$

where the nuclear-relaxed exciton energy ϵ_μ is defined as

$$\epsilon_\mu = E_\mu - \sum_k G_k^{\mu\mu 2}/(\hbar\omega_k). \tag{15}$$

The renormalized perturbative Hamiltonian $V^R(t)$ is defined as

$$V^R(t) = \sum_{\mu\nu}^{\mu\neq\nu}[v_{q\mu\nu} - v_{c\mu\nu}(t,t')]|\mu\rangle\langle\nu|, \tag{16}$$

$$v_{q\mu\nu} \equiv \theta_\mu B_{\mu\nu}\theta_\nu^\dagger, \tag{17}$$

where θ_μ is expressed as $e^{S_{\mu\mu}}$.

We now derive the rate formula for the transition between off-diagonal elements. By using the new bracket, we define function $v_c(t_1,t)$ in single integration as

$$\langle 1, v_{cI}(t_1,t)\rangle_t = \langle 1, v_{qI}(t_1)\rangle_t, \tag{18}$$

$$\langle v_{cI}^\dagger(t_1,t), 1\rangle_t = \langle v_{qI}^\dagger(t_1), 1\rangle_t, \tag{19}$$

where we introduce the interaction representation of $v_c(t_1,t)$ and v_q as $v_{cI}(t_1,t) \equiv U^\dagger(t_1)v_c(t_1,t)U(t_1)$ and $v_{qI}(t_1) \equiv U^\dagger(t_1)v_qU(t_1)$.

2.4. General Rate Formula

According to the Appendix, the term of the single integration becomes zero. Then, inserting $v_q - v_c(t)$ into $V(t)$, we obtain the reduced density matrix of Eq. (11) as

$$\rho(t) = \langle 1,1\rangle_t + \frac{1}{\hbar^2}\int_0^t dt_1 \int_0^t dt_1' M_{ff'ii'}(t_1,t_1'), \tag{20}$$

where we define the memory kernel as

$$M_{ff'ii'}(t_1,t_1') \equiv \langle v_{qI}^\dagger(t_1'), v_{qI}(t_1)\rangle_t - \langle v_{cI}^\dagger(t_1',t), v_{cI}(t_1,t)\rangle_t. \tag{21}$$

Using the expression

$$U(t) \equiv u_b(t)\sum_\alpha u_\alpha(t)|\alpha\rangle\langle\alpha| \equiv u_b(t)u_e(t), \tag{22}$$

where $u_b(t)$ is the propagator of the bath defined as $e^{-iH_bt/\hbar}$, and $u_e(t)$ is the propagator of the renormalized electronic exciton state, defined as

$$\langle\alpha(0)|u_e(t)|\mu\rangle = \exp\left[-\frac{i}{\hbar}\int_0^t d\tau\epsilon_\alpha(\tau)\right]\langle\alpha(0)|\mu\rangle. \tag{23}$$

Then, we finally obtain the time-dependent renormalized second-order perturbation term of the memory kernel as

$$M_{ff'ii'}(t_1,t_1') \equiv \sum_{\mu\mu'\nu\nu'} R_{ff'ii'}^{\mu\mu'\nu\nu'}(t_1,t_1')G_{\mu\mu'\nu\nu'}^{ff'ii'}(t_1,t_1'), \tag{24}$$

where function $R_{ff'ii'}^{\mu\mu'\nu\nu'}(t_1,t_1')$ is defined as follows:

$$R_{ff'ii'}^{\mu\mu'\nu\nu'}(t_1,t_1') = \langle i'|u_e^\dagger(t_1')|\nu'\rangle\langle\mu'|u_e^\dagger(t)u_e(t_1')|f'\rangle \times\langle f|u_e^\dagger(t_1)u_e(t)|\mu\rangle\langle\nu|u_e(t_1)|i\rangle e^{W(t_1,t_1')+W_{\mu\nu}(t_1,t_1')+W_{\mu'\nu'}^\dagger(t_1,t_1')}. \tag{25}$$

Furthermore, the function $G_{\mu\mu'\nu\nu'}^{ff'ii'}(t_1,t_1')$ is defined as follows:

$$G_{\mu\mu'\nu\nu'}^{ff'ii'}(t_1,t_1') = e^{P_{\mu\mu'\nu\nu'}(t_1,t_1')}[Q_{\mu\mu'\nu\nu'}(t_1,t_1') + (X_{\mu'\nu'}^\dagger(t_1,t_1') + Y_{\mu\mu'\nu\nu'}^\dagger(t_1,t_1'))(X_{\mu\nu}(t_1,t_1') + Y_{\mu\mu'\nu\nu'}(t_1,t_1'))] - X_{\mu'\nu'}^\dagger(t_1,t_1')X_{\mu\nu}(t_1,t_1'). \tag{26}$$

The details of P, Q, W, X, and Y are provided in the Appendix.

Consequently, we define the time-dependent relaxation rate $k_{ff'ii'}(t)$, which is the time-dependent Redfield tensor in the dissipation term of the quantum master equation. Differentiating Eq. (20) by time t, we obtain

$$\frac{\partial\rho(t)}{\partial t} = \frac{i}{\hbar}(\langle H_0^R(t),1\rangle_t - \langle 1, H_0^R(t)\rangle_t) + k_{ff'ii'}(t). \tag{27}$$

Hence, the time-dependent rate is expressed as

$$k_{ff'ii'}(t) = \frac{1}{\hbar^2}\int_0^t dt_1[M_{ff'ii'}(t,t_1) + M_{ff'ii'}(t_1,t)], \tag{28}$$

where we assume that the differentiation term for the variable of time t in the memory kernel can be neglected because its term is neglected for the MRT. In the case without renormalization approach as $v_{c\mu\nu}(t,t') = 0$ in Eq. (16), the rate formula of the modified redfield theory is reproduced by Eq. (28) in the limit of $t\to\infty$ as $i' = i$ and $f' = f$.

By using the analytical expression of the memory kernel $M_{ff'ii'}(t_1,t_1')$, we can calculate the dissipation term of the quantum master equation for site representation. In order to numerically compare the time-dependent rate $k_{ff'ii'}(t)$ for delocalized representation and that for site representation, the relaxation rate for site representation is defined as

$$k_{mm'nn'}^{site}(t) = \sum_{ff'ii'} C_n^i C_{n'}^{i'} C_m^f C_{m'}^{f'} k_{ff'ii'}(t). \tag{29}$$

3. Numerical Analysis

In order to check the refinement of TRRT, we numerically analyzed the time-dependent reaction rates for two molecular systems, and show the results through two electronic representations: one was based on delocalized exciton states from the upper energy exciton state $|+\rangle$ to the lower state $|-\rangle$, whereas the other was based on on localized exciton states, from the excited donor (site 1) state $|1\rangle$ to the excited acceptor (site 2) state $|2\rangle$.

In this letter, we used the density of states for nuclear vibrations defined as $J_{mn}(\omega) = \sum_k g_{mk}g_{nk}\omega_k^2\delta(\omega-\omega_k)$ as super-ohmic-type, which is proportional to $(\lambda\omega^3/2\omega_c^3)e^{-\omega/\omega_c}$, where ω_c is the cutoff frequency. In the following, all parameters were normalized to the cutoff energy of the phonon as $\hbar\omega_c$. In addition, we neglected the correlation in nuclear fluctuation between each pair of localized exciton states $|m\rangle$ and $|n\rangle$ as $J_{nm}(\omega) = \delta_{mn}J_m(\omega)$.

The temporal dependencies of the reaction rate $k_{--++}(t)$ and $k_{2211}^{site}(t)$ using MRT and TRRT are shown in Fig. 1, where the parameters are $V_{12}^e/\hbar\omega_c = 1$, $\beta/\hbar\omega_c = 1$, $\Delta E/\hbar\omega_c = 1$, and

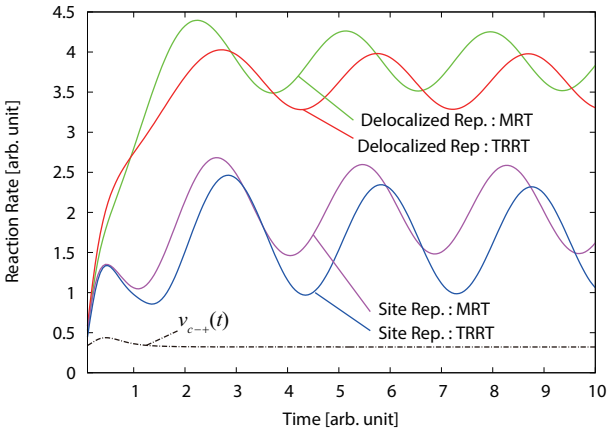

Figure 1: Time dependencies of the reaction rates. Relaxation rate $k_{--++}(t)$ from the upper-exciton state to the lower-exciton state by MR and TRRT. Exciton relaxation rate $k^{site}_{2211}(t)$ for the site representation from site 1 to site 2 by MR and TRRT. The degree of the off-diagonal element of $v_{c-+}(t)$. Other parameters were $V^e_{12}/\hbar\omega_c = 1, \beta/\hbar\omega_c = 1, \Delta E/\hbar\omega_c = 1$, and $\lambda/\hbar\omega_c = 1$.

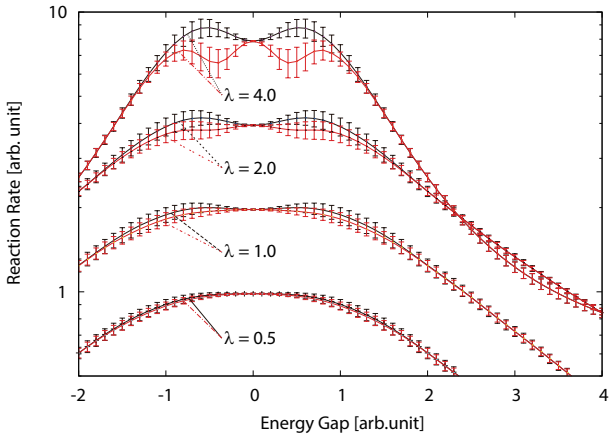

Figure 2: Energy gap dependency of the average relaxation rate $\bar{k}_{--++}$ and its fluctuation Δk_{--++} from upper state $|+\rangle$ to the lower state $|-\rangle$ in delocalized exciton representation by MR (black curves) and TRRT (red curves). The energy gap was defined as $\Delta E = E_1 - E_2$. The values of the reorganization energy varied from 0.5 to 4.0. Other parameters were $V^e_{12}/\hbar\omega_c = 1$, and $\beta\hbar\omega_c = 1.0$.

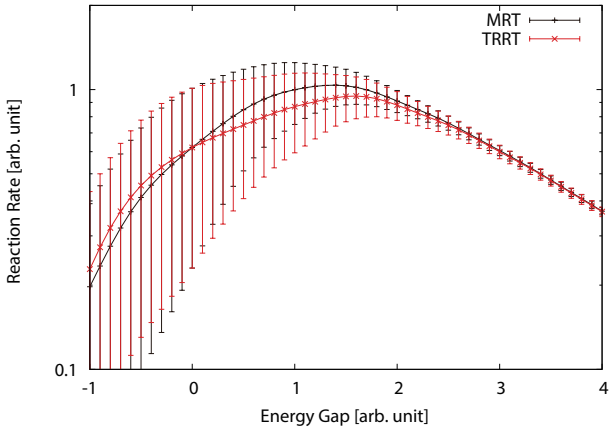

Figure 3: Energy gap dependency of the average relaxation rate $\bar{k}^{site}_{2211}$ and its fluctuation Δk_{2211} for site representation from site 1 to site 2 by MR and TRRT. The energy gap was defined as $\Delta E = E_1 - E_2$. Other parameters were $V^e_{12}/\hbar\omega_c = 1$, $\lambda/\hbar\omega_c = 1.0$, and $\beta\hbar\omega_c = 1.0$.

$\lambda/\hbar\omega_c = 1$, and ΔE is the energy gap for site representation as $E_1 - E_2$. While the value of v_c varied in the short-time region, the reaction rates for each representation drastically increased, and the properties due to TRRT were slightly different from that due to MRT. For the temporal region longer than the nuclear-vibrational relaxation time by approximately $1/\omega_c$, the rate by using MRT and TRRT coherently fluctuated, but the average values were different. In particular, the average rate using TRRT was smaller than that using MRT. Moreover, the phases for each theory relatively shifted. We then estimated the average rate $\bar{k}_{ff'ii'}$ and its dispersion $\Delta k_{ff'ii'}$ defined as

$$\bar{k}_{ff'ii'} = \int_{T_{min}}^{T_{max}} \frac{k_{ff'ii'}(t)}{T_{max} - T_{min}} dt, \tag{30}$$

$$(\Delta k_{ff'ii'})^2 = \int_{T_{min}}^{T_{max}} \frac{(k_{ff'ii'}(t) - \bar{k}_{ff'ii'})^2}{T_{max} - T_{min}} dt, \tag{31}$$

where the time regions are determined as $\omega_c T_{min} = 2.0$, $\omega_c T_{max} = 10.0$.

Because we found some bugs in the program we used for the numerical calculation of the time-dependent rate in the previous letter, we recalculated the energy gap dependencies of the average relaxation rate $\bar{k}_{--++}$ and the dispersion of its fluctuation Δk_{--++} from the upper state to the lower state by using MRT and the TRRT, as shown in Fig. 2. For all regions with an energy gap, the rate by using TRRT was smaller than that by MRT. When the reorganization energy increased in magnitude, three peaks appeared in Fig. 2. With a peak for the case where $\Delta E = 0$, the system was resonant immediately after photoexcitation. The cause of the other peaks might have been the resonant case where $|\Delta E| \simeq \hbar\omega_c$. In the region of the energy gap between $0 < |\Delta E| < \hbar\omega_c$, the rate by TRRT was smaller than that by MRT due to the renormalization effect.

The energy gap dependencies of the average relaxation rate $\bar{k}^{site}_{2211}$ and the dispersion of its fluctuation Δk_{2211} for the site representation from site 1 to site 2 by MRT and TRRT are shown in Fig. 3. When the energy gap was zero, the value of the averaged rate by MRT equaled that by TRRT. For the region with a positive energy gap, the averaged rate by TRRT was smaller than that by MRT. Although the differences between MRT and TRRT were small in the case of small reorganization energy value λ in Fig. 4, the differences in the case of large reorganization energy values became apparent. When the reorganization energy became large, two peaks appeared. Although the energy gap dependence for relaxation from the upper delocalized exciton state to the lower was symmetrical, the relaxation rate for the site representation was not. When the energy gap ΔE was zero, the results by TRRT were equal to those by MRT due to the resonance case. Thus, by considering the thermalization effect, the reduction in the relaxation rate occurs. When ΔE becomes large again, the system might become resonant again. Consequently, a second peak of the relaxation rate might emerge.

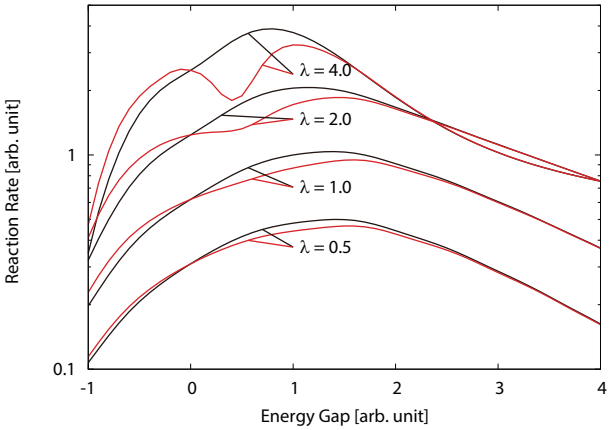

Figure 4: Energy gap dependency of the averaged relaxation rate $\bar{k}^{site}_{2211}$ for site representation from site 1 to site 2 by MR (black curves) and TRRT (red curves). The energy gap was defined as $\Delta E = E_1 - E_2$. The value of the reorganization energy varied from 0.5 to 4.0. Other parameters were $V^e_{12}/\hbar\omega_c = 1$, and $\beta\hbar\omega_c = 1.0$.

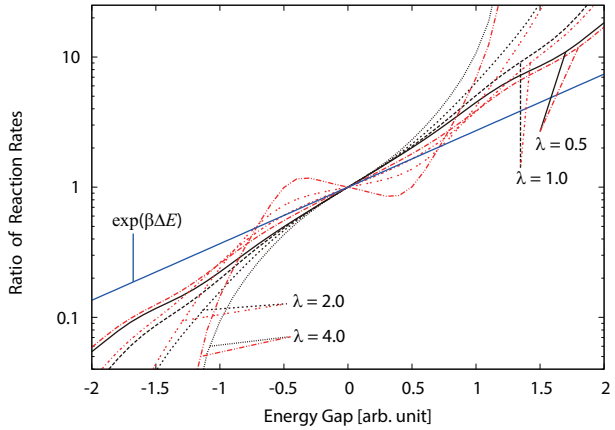

Figure 5: Energy gap dependency of the ratio of forward ($|1\rangle \rightarrow |2\rangle$) to backward ($|2\rangle \rightarrow |1\rangle$) average relaxation rates for site representation by using MR (black curves) and TRRT (red curves). The energy gap was defined as $\Delta E = E_1 - E_2$. The value of the reorganization energy was varied from 0.5 to 4.0. The straight line was $\exp(\beta\Delta E)$.

4. Discussion

The qualitative refinement was due to the renormalization of the time-dependent perturbative interaction term. The renormalization approach perfectly deletes the first-order perturbation term of the reduced density matrix. This term represents the degree of quantum mechanical interference between pure exciton states. Thus, one physical reason for the difference between the results by TRRT and MRT means that the rate obtained by using TRRT included interference effects. The second-order perturbation term of the reduced density matrix was expressed by the form of the variance-covariance matrix. Thus, the TRRT is applicable to any value of reorganization energy, but is dependent on the degree of the elements in the variance-covariance matrix for exciton-phonon interaction.

The relaxation rate obtained by using TRRT for the site representation was larger than that by MRT. We analyzed how the detailed balance between MRT and TRRT was satisfied. Fig. 5 shows the energy gap dependence of the ratio between forward and backward relaxation rates as $\bar{k}^{site}_{2211}/\bar{k}^{site}_{1122}$. It is apparent that the curve by TRRT is more similar to $\exp(\beta\Delta E)$ than that by MRT, although the curve obtained by using TRRT in the case of large reorganization energy fluctuated about $\exp(\beta\Delta E)$. This property might have occurred due to the large variance about nuclear fluctuations in exciton states due to the large reorganization energy. The difference between TRRT and $\exp(\beta\Delta E)$ might have been due to different thermal equilibrium states in the steady state, although the TRRT yielded correct result for the transient reaction process immediately following photo-excitation. On the contrary, it is known that exitonic equilibrium holds for lamda approaching zero [17, 18]. It may not be suitable that this energy gap is a good parameter for defining thermal equilibrium populations. We hence might need to consider the delocalized exciton gap, and thermal renormalization effects might provide better evaluation of the performance of the new method.

The temperature dependence of the size of exciton delocalization in Photosystem II (PSII) was recently studied by using the variational master equation (VME) [19]. In the intermediate coupling case excluding the relatively large energy gap, as $\lambda \sim |V^e_{12}| < |\Delta E|$ in some chlorophyll pairs in the PSII, the results showed that the EET mechanism by using the VME was of the Förster type. On the contrary, the result obtained by numerically exact calculations[20] yielded a Redfield-type mechanism. In the intermediate coupling region, there were local minima for the numerical analysis of free energy analysis in the VME [21–23]. These variational parameters included both delocalized and localized exciton states [19, 21, 24]. In case of strong excitonic coupling, the numerically calculated rate was lower than that obtained by numerically exact analysis. In such situations, when we selected the other solution of the variational parameter, we could have reproduced the result of the numerically exact calculation[23]. Although the cause of the reproduction was not apparent, we intend to apply TRRT to study it with the upper limit of the Bogoliubov inequality for free energy.

Finally, the analysis of quantum coherence via nuclear vibrations in the photosynthetic antenna systems have recently been proposed using polaron formation [21, 25, 26] as well as modifications based on variational approaches [27–29]. In future work, to compare these theories, we need a comprehensive comparison with simple Redfield, Förster, or VME methods at least, because the parameter regimes examined in this work might not rest in the range where the MRT yields good results.

5. Conclusion

In this letter, we formulated the time-dependent rate for the transition between off-diagonal elements by introducing a time-dependent renormalization technique based on the MRT. By numerical analysis, we found that the average rate by using TRRT for site representation was slower than that by MRT for the case where $\Delta E > 0$, although the time dependence of the reaction rate oscillated in the intermediate coupling case. This result is consistent with that in our previous study. For the case where

$\Delta E < 0$, we found that the average rate obtained by using TRRT was slightly larger than that by using MRT. By comparing the ratio of the rates for the forward and backward reactions, we found that the TRRT has a property which approaches the theorem of detailed balance more closely than the result obtained by using MRT. We believe the theoretical development in this letter will raise questions about the relationship between high yields and the quantum effects in light harvesting systems in photosynthetic reactions.

Appendix A. Expression of v_c

According to the definitions of Eqs. (18) and (19), let us consider the term as

$$\begin{aligned}&\langle 1, v_{cI}(t_1,t)\rangle_t \\ &= \sum_{\alpha\alpha'} u^*_{e,\alpha}(t_1)u_{e,\alpha'}(t_1)\langle\alpha|v_c(t_1,t)|\alpha'\rangle\langle 1,|\alpha\rangle\langle\alpha'|\rangle_t, \qquad \text{(A.1)}\\ &\langle 1, v_{qI}(t_1)\rangle_t \\ &= \sum_{\alpha\alpha'} u^*_{e,\alpha}(t_1)u_{e,\alpha'}(t_1)\langle 1,|\alpha\rangle\langle\alpha|v_q(t_1)|\alpha'\rangle\langle\alpha'|\rangle_t, \qquad \text{(A.2)}\end{aligned}$$

where we introduce the exciton-phonon interaction for interaction representation by nuclear fluctuation as $v_q(t) \equiv u_b^\dagger(t)v_q u_b(t)$.

Based on the definition of v_c, let us express the matrix element of v_c as a simple relation as

$$\langle\alpha|v_c(t_1,t)|\alpha'\rangle\langle 1,|\alpha\rangle\langle\alpha'|\rangle_t = \langle 1,|\alpha\rangle\langle\alpha|v_q(t_1)|\alpha'\rangle\langle\alpha'|\rangle_t. \qquad \text{(A.3)}$$

Then, the l.h.s of Eq. (A.3) can be expressed as

$$\begin{aligned}&\sum_\beta \langle i'|\beta\rangle\langle\beta|f'\rangle u^*_\beta(t)\langle f|\alpha\rangle\langle\alpha'|i\rangle u_\alpha(t) \\ &\times\langle\alpha|v_c(t_1,t)|\alpha'\rangle \mathrm{Tr}[\theta^\dagger_{i'}\theta_{f'}(t)\theta^\dagger_f(t)\theta_i\rho_b], \qquad \text{(A.4)}\end{aligned}$$

where we introduce the shift operator for interaction representation by nuclear fluctuation as $\theta_i(t) \equiv u_b^\dagger(t)\theta_i u_b(t)$. The r.h.s of Eq. (A.3) can then be expressed as

$$\begin{aligned}&\sum_\beta \langle i'|\beta\rangle\langle\beta|f'\rangle u^*_\beta(t)\langle f|\alpha\rangle\langle\alpha'|i\rangle u_\alpha(t) \\ &\times \mathrm{Tr}[\theta^\dagger_{i'}\theta_{f'}(t)\theta^\dagger_f(t)\langle\alpha|v_q(t_1)|\alpha'\rangle\theta_i\rho_b]. \qquad \text{(A.5)}\end{aligned}$$

Thus, transferring representation α into the pure exciton representation μ, we obtain

$$\begin{aligned}\langle\mu|v_c(t_1,t)|\nu\rangle &= \frac{\mathrm{Tr}[\theta^\dagger_{i'}\theta_{f'}(t)\theta^\dagger_f(t)\langle\mu|v_q(t_1)|\nu\rangle\theta_i\rho_b]}{\mathrm{Tr}[\theta^\dagger_{i'}\theta_{f'}(t)\theta^\dagger_f(t)\theta_i\rho_b]} \\ &= X_{\mu\nu}(t_1,t_1')e^{W_{\mu\nu}}(t_1,t_1'). \qquad \text{(A.6)}\end{aligned}$$

The Hermite conjugate $\langle\mu|v_c^*(t_1,t)|\nu\rangle$ is expressed by taking its Hermite conjugation and exchanging the indices with each other, as $i \leftrightarrow i'$ and $f \leftrightarrow f'$.

Appendix B. Correlation function

Using Eq. (A.6), we can find

$$\begin{aligned}\langle v^\dagger_{cI}(t_1',t), v_{cI}(t_1,t)\rangle_t &= \mathrm{Tr}[\theta^\dagger_{i'}u_b^\dagger(t)\theta_{f'}\theta^\dagger_f u_b(t)\theta_i\rho_b] \\ &\times\sum_{\mu\nu}\langle f|u_e^\dagger(t_1)u_e(t)|\mu\rangle\langle\mu|v_c(t_1,t)|\nu\rangle\langle\nu|u_e(t_1)|i\rangle \\ &\times\sum_{\mu'\nu'}\langle i'|u_e^\dagger(t_1')|\nu'\rangle\langle\nu'|v_c^\dagger(t_1,t)|\mu'\rangle\langle\mu'|u_e^\dagger(t)u_e(t_1')|f'\rangle. \qquad \text{(B.1)}\end{aligned}$$

In addition to this relation, $\langle v^\dagger_{cI}(t_1',t), v_{qI}(t_1)\rangle_t$ and $\langle v^\dagger_{qI}(t_1'), v_{cI}(t_1,t)\rangle_t$ are equal to $\langle v^\dagger_{cI}(t_1',t), v_{cI}(t_1,t)\rangle_t$.

The second order of v_q is expressed as

$$\begin{aligned}&\langle U^\dagger(t_1')v_q^\dagger U(t_1'), U^\dagger(t_1)v_q U(t_1)\rangle_t \\ &= \sum_{\mu\mu'\nu\nu'}\langle i'|u_e^\dagger(t_1')|\nu'\rangle\langle\nu|u_e(t_1)|i\rangle\langle f|u_e^\dagger(t_1)u_e(t)|\mu\rangle\langle\mu'|u_e^\dagger(t)u_e(t_1')|f'\rangle \\ &\times\mathrm{Tr}[\theta^\dagger_{i'}\langle\nu'|v_q^\dagger(t_1')|\mu'\rangle\theta_{f'}(t)\theta^\dagger_f(t)\langle\mu|v_q(t_1)|\nu\rangle\theta_i\rho_b]. \qquad \text{(B.2)}\end{aligned}$$

Consequently, we can obtain the time correlation as

$$\begin{aligned}&\langle(v^\dagger_{qI}(t_1') - v^\dagger_{cI}(t_1',t)), (v_{qI}(t_1) - v_{cI}(t_1,t))\rangle_t \\ &= \langle v^\dagger_{qI}(t_1'), v_{qI}(t_1)\rangle_t - \langle v^\dagger_{cI}(t_1',t), v_{cI}(t_1,t)\rangle_t. \qquad \text{(B.3)}\end{aligned}$$

Appendix C. Calculation of correlation

In this section, we state the general method for the expressions of the correlation functions as the denominator and the numerator of the r.h.s in Eq. (A.6). In addition, we need to analyze the following correlation regarding the first term on the r.h.s of Eq. (B.3):

$$\begin{aligned}&\mathrm{Tr}[\theta^\dagger_{i'}\theta_{\nu'}(t_1')B^\dagger_{\nu'\mu'}(t_1')\theta^\dagger_{\mu'}(t_1')\theta_{f'}(t) \\ &\times\theta^\dagger_f(t)\theta_\mu(t_1)B_{\mu\nu}(t_1)\theta^\dagger_\nu(t_1)\theta_i\rho_b], \qquad \text{(C.1)}\end{aligned}$$

where $\theta_\mu = e^{S_{\mu\mu}}$, and $S_{\mu\mu} = \sum_k \frac{G_k^{\mu\mu}}{\hbar\omega_k}(b_k^\dagger - b_k)$.

In order to do this, we simply analyze the following operator as

$$e^A Be^C De^E = \partial_x\partial_y e^A e^{xB}e^C e^{yD}e^E|_{x=y=0}, \qquad \text{(C.2)}$$

where A, B, C, D, and E are linear combinations of the creation and the annihilation operators of the phonon. For example, in Eq. (C.1) they are as follows:

$$\begin{aligned}A &= -S_{i'i'}(0) + S_{\nu'\nu'}(t_1'),\\ B &= B^\dagger_{\nu'\mu'}(t_1'),\\ C &= -S_{\mu'\mu'}(t_1') + S_{f'f'}(t) - S_{ff}(t) + S_{\mu\mu}(t_1),\\ D &= B_{\mu\nu}(t_1),\\ E &= -S_{\nu\nu}(t_1) + S_{ii}(0). \qquad \text{(C.3)}\end{aligned}$$

By using the relation as $e^Ae^B = e^{A+B+\frac{1}{2}[A,B]}$, we obtain

$$\begin{aligned}\langle e^A e^{xB}e^C e^{yD}e^E\rangle =& e^{\frac{1}{2}[A+xB,xB+C]+\frac{1}{2}[C+yD,yD+E]+\frac{1}{2}[A+xB,yD+E]} \\ &\times e^{\frac{1}{2}\langle(A+xB+C+yD+E)^2\rangle}. \qquad \text{(C.4)}\end{aligned}$$

Differentiating it by x and y, and inserting $x = y = 0$, we obtain

$$\begin{aligned}\partial_x\partial_y\langle e^A e^{xB} e^C e^{yD} e^E\rangle|_{x=y=0} &= e^{\frac{1}{2}(\langle AA\rangle+\langle CC\rangle+\langle EE\rangle+2\langle AC\rangle+2\langle CE\rangle+2\langle AE\rangle)} \\ &\times [\langle BD\rangle + (\langle DE\rangle + \langle AD\rangle + \langle CD\rangle) \\ &\times (\langle BC\rangle + \langle BE\rangle + \langle AB\rangle)]. \qquad \text{(C.5)}\end{aligned}$$

Appendix D. Introducing the correlation function for monomers

We express the correlation function by the shift operator $S_{\mu\nu}$ under a delocalized representation as the following inner product:

$$\begin{aligned}\langle S_{\mu\nu}(t) S_{\mu'\nu'}(t')\rangle &= \sum_{nm} C_n^\mu C_n^\nu C_m^{\mu'} C_m^{\nu'} \gamma_{nm}(t-t') \\ &= \boldsymbol{c}_{\mu\nu}\gamma(t-t')\boldsymbol{c}_{\mu'\nu'}, \qquad \text{(D.1)}\end{aligned}$$

where $\boldsymbol{c}_{\mu\nu}$ and $\gamma_{nm}(t)$ are defined as

$$(\boldsymbol{c}_{\mu\nu})_n \equiv C_n^\mu C_n^\nu, \qquad \text{(D.2)}$$

$$\gamma_{nm}(t) = \sum_k \frac{g_{nk}g_{mk}}{\hbar^2\omega_k^2}[-2(n_k+\frac{1}{2})\cos(\omega_k t) + i\sin(\omega_k t)]. \qquad \text{(D.3)}$$

Appendix E. Summary of correlation functions

Finally, we show the functions of W, P, Q, X, and Y as

$$\begin{aligned}W(t_1,t_1') &= (\boldsymbol{c}_{i'i'} - \boldsymbol{c}_{ii})\gamma(0)(\boldsymbol{c}_{i'i'} - \boldsymbol{c}_{ii})/2 \\ &+ (\boldsymbol{c}_{f'f'} - \boldsymbol{c}_{ff})\gamma(0)(\boldsymbol{c}_{f'f'} - \boldsymbol{c}_{ff})/2 \\ &- \boldsymbol{c}_{i'i'}\gamma(-t)(\boldsymbol{c}_{f'f'} - \boldsymbol{c}_{ff}) \\ &+ (\boldsymbol{c}_{f'f'} - \boldsymbol{c}_{ff})\gamma(t)\boldsymbol{c}_{ii}, \qquad \text{(E.1)}\\ W_{\mu\nu}(t_1,t_1') &= (\boldsymbol{c}_{\nu\nu} - \boldsymbol{c}_{\mu\mu})[\gamma(0)(\boldsymbol{c}_{\nu\nu} - \boldsymbol{c}_{\mu\mu})/2 - \gamma(t_1)\boldsymbol{c}_{ii} \\ &+ \gamma(-t_1)\boldsymbol{c}_{i'i'} - \gamma(t-t_1)(\boldsymbol{c}_{f'f'} - \boldsymbol{c}_{ff})], \qquad \text{(E.2)}\\ W^\dagger_{\mu'\nu'}(t_1,t_1') &= (\boldsymbol{c}_{\nu'\nu'} - \boldsymbol{c}_{\mu'\mu'})[\gamma(0)(\boldsymbol{c}_{\nu'\nu'} - \boldsymbol{c}_{\mu'\mu'})/2 + \gamma(t_1')\boldsymbol{c}_{ii} \\ &- \gamma(-t_1')\boldsymbol{c}_{i'i'} + \gamma(t_1'-t)(\boldsymbol{c}_{f'f'} - \boldsymbol{c}_{ff})], \qquad \text{(E.3)}\end{aligned}$$

$$\begin{aligned}P_{\mu\mu'\nu\nu'}(t_1,t_1') &= (\boldsymbol{c}_{\mu'\mu'} - \boldsymbol{c}_{\nu'\nu'})\gamma(t_1'-t_1)(\boldsymbol{c}_{\nu\nu} - \boldsymbol{c}_{\mu\mu}), \qquad \text{(E.4)}\\ Q_{\mu\mu'\nu\nu'}(t_1,t_1') &= \hbar^2\boldsymbol{c}_{\nu'\mu'}\ddot{\gamma}(t_1'-t_1)\boldsymbol{c}_{\nu\mu}, \qquad \text{(E.5)}\end{aligned}$$

$$\begin{aligned}X_{\mu\nu}(t_1,t_1') &= i\hbar\boldsymbol{c}_{\mu\nu}[\dot{\gamma}(0)\boldsymbol{c}_{\nu\nu} + \dot{\gamma}^*(0)\boldsymbol{c}_{\mu\mu} \\ &- \dot{\gamma}(t_1)\boldsymbol{c}_{ii} - \dot{\gamma}^*(t_1)\boldsymbol{c}_{i'i'} \\ &+ \dot{\gamma}^*(t_1-t)(\boldsymbol{c}_{f'f'} - \boldsymbol{c}_{ff})], \qquad \text{(E.6)}\\ X^\dagger_{\mu'\nu'}(t_1,t_1') &= i\hbar\boldsymbol{c}_{\nu'\mu'}[-\dot{\gamma}(t_1'-t)(\boldsymbol{c}_{f'f'} - \boldsymbol{c}_{ff}) \\ &+ \dot{\gamma}(0)\boldsymbol{c}_{\mu'\mu'} + \dot{\gamma}^*(0)\boldsymbol{c}_{\nu'\nu'} \\ &- \dot{\gamma}(t_1')\boldsymbol{c}_{ii} - \dot{\gamma}^*(t_1')\boldsymbol{c}_{i'i'}], \qquad \text{(E.7)}\end{aligned}$$

$$\begin{aligned}Y_{\mu\mu'\nu\nu'}(t_1,t_1') &= i\hbar\boldsymbol{c}_{\nu\mu}\dot{\gamma}^*(t_1-t_1')(\boldsymbol{c}_{\nu'\nu'} - \boldsymbol{c}_{\mu'\mu'}), \qquad \text{(E.8)}\\ Y^\dagger_{\mu\mu'\nu\nu'}(t_1,t_1') &= -i\hbar\boldsymbol{c}_{\nu'\mu'}\dot{\gamma}(t_1'-t_1)(\boldsymbol{c}_{\mu\mu} - \boldsymbol{c}_{\nu\nu}), \qquad \text{(E.9)}\end{aligned}$$

where dot implies the time derivative of the function.

[1] H. van Amerongen, L. Valkunas, R. van Grondelle, Photosynthetic Excitons, World Scientific, Singapore, 2000.
[2] N. Lambert, Y.-N. Chen, Y.-C. Cheng, C.-M. Li, G.-Y. Chen, F. Nori, Nat. Phys. 9 (2013) 10.
[3] S. F. Huelga, M. B. Plenio, Contemp. Phys. 54 (4) (2013) 181.
[4] D. Abramavicius, L. Valkunas, Photosynth. Res. 127 (2016) 33.
[5] T. Förster, Ann. Phys. (Leipzig) 437 (1948) 55.
[6] A. G. Redfield, IBM J. Res. Dev. 1 (1957) 19.
[7] V. May, O. Kühn, Charge and Energy Transfer Dynamics in Molecular Systems, 3rd Edition, WILEY-VCH Verlag GmbH & Co. KGaA, Germany, 2011.
[8] W. M. Zhang, T. Meier, V. Chernyak, S. Mukamel, J. Chem. Phys. 108 (1998) 7763.
[9] M. Yang, G. R. Fleming, Chem. Phys. 275 (2002) 355.
[10] Y.-H. Hwang-Fu, W. Chen, Y.-C. Cheng, Chem. Phys. 447 (2015) 46.
[11] Y. Chang, Y.-C. Cheng, J. Chem. Phys. 142 (2015) 034109.
[12] M.-J. Tao, Q. Ai, F.-G. Deng, Y.-C. Cheng, Sci. Rep. 6 (2016) 27535.
[13] A. Kimura, Chem. Phys. Lett. 645 (2016) 123.
[14] S. Nakajima, Prog. Theo. Phys. 20 (1958) 948.
[15] R. Zwanzig, J. Chem. Phys. 33 (1960) 1338.
[16] H.-P. Breuer, F. Petruccione, The Theory of Open Quantum Systems, Oxford University Press, Oxford, 2002.
[17] A. Gelzinis, D. Abramavicius, L. Valkunas, Phys. Rev. B 84 (2011) 245430.
[18] J. M. Moix, Y. Zhao, J. Cao, Phys. Rev. B 85 (2012) 115412.
[19] Y. Fujihashi, A. Kimura, J. Phys. Chem. B 119 (2015) 8349.
[20] A. Ishizaki, G. R. Fleming, J. Chem. Phys. 130 (2009) 234111.
[21] D. P. S. McCutcheon, A. Nazir, J. Chem. Phys. 135 (2011) 114501.
[22] Y. Fujihashi, A. Kimura, J. Phys. Soc. Japan 83 (2014) 014801.
[23] A. Kimura, Y. Fujihashi, J. Chem. Phys. 141 (2014) 194110.
[24] D. Čevizović, Z. Ivić, S. Galović, A. Reshetnyak, A. Chizhov, Physica B: Cond. Matt. 490 (2016) 9.
[25] S. Jang, Y.-C. Cheng, D. R. Reichman, J. D. Eaves, J. Chem. Phys. 129 (2008) 101104.
[26] S. Jang, J. Chem. Phys. 135 (2011) 034105.
[27] D. Chen, J. Ye, H. Zhang, Y. Zhao, J. Phys. Chem. B 115 (2011) 5312.
[28] V. Chorosajev, A. Gelzinis, L. Valkunas, D. Abramavicius, J. Chem. Phys. 140 (2014) 244108.
[29] V. Chorosajev, O. Rancova, D. Abramavicius, Phys. Chem. Chem. Phys. 18 (2016) 7966.